General Fishnet Statistics of Strength: Nacreous, Biomimetic, Concrete, Octet-Truss, and Other Architected or Quasibrittle Materials

Wen Luo
Department of Civil and Environmental Engineering,
Northwestern University,
Evanston, IL 60208
e-mail: wenluo2016@u.northwestern.edu

Zdeněk P. Bažant[1]
McCormick Institute Professor and W.P. Murphy Professor of Civil and Mechanical Engineering and Materials Science,
Northwestern University,
2145 Sheridan Road, CEE/A135,
Evanston, IL 60208
e-mail: z-bazant@northwestern.edu

The fishnet probabilistic model was recently developed to characterize the strength distribution of nacre-like biomimetic materials. It reveals that the unique fishnet-like connectivity of the material microstructure brings about enormous safety gain at the extremely low failure probability level of one out of a million, desired for engineering structures. The gist of the theory is that the material microstructure plays a determining role in its failure probability tail. Therefore, a carefully designed connectivity for a material microstructure not only enhances its mean strength but also significantly reduces its marginal failure risk. Here, we first show that the initially introduced series expansion and the newer formulation based on order statistics are, in the fishnet model, essentially equivalent. From that we develop a neat general form of the fishnet statistics. Then, we extend our theoretical approach to the strength distributions of architected nanomaterials such as the printed octet-truss carbon nanolattices, as well as to quasibrittle particulate composites such as concrete, and formulate a unified general fishnet statistics. We demonstrate that the octet-truss system can be physically seen and statistically treated as a union of three fishnets with three mutually orthogonal orientations. We show that the three-dimensional assembly of fishnets further enhances the tail strength at the 10^{-6} probability quantile, compared to two-dimensional (2D) fishnet statistics. We compare the performance of different statistical strength models by fitting of the simulated and experimental histograms data for the octet-truss nanolattice. Finally, we argue that, at the extreme lower tail of failure probability, quasibrittle materials such as concrete or fiber composites should partially exhibit the fishnet-type statistical behavior. [DOI: 10.1115/1.4045589]

Keywords: computational mechanics, failure criteria, mechanical properties of materials, micromechanics, stress analysis, structures

1 Introduction

Material scientists and engineers developing new engineering structures and materials have been focusing mainly on enhancing the mean strength, while the extreme lower tail of the strength distribution $P_f(\sigma)$ has long been ignored. However, the consensus of safety experts [1,2] is that engineering structures must be designed with failure probability not exceeding 10^{-6} so that engineers do not add appreciably to the risks people inevitably face (the risk of dying in a car accident is, in the US, about 1 in a hundred per lifetime, while 1 in a million is the risk of death by lightning, or by a falling tree, or by a fall in the bathroom). Maximizing the mean strength is not enough. It can even happen that a material or structure of a lower mean strength would have, for the same coefficient of variation, a higher tail strength at 10^{-6} and vice versa (see Fig. 6). Therefore, a realistic probabilistic model for structure strength is necessary.

The amazing strength of bioinspired hierarchical materials such as nacre [3,4] and shell of conch [5], which is about ten times greater than the strength of its main constituent, have been extensively researched over the past two decades. Studies of the toughening mechanism engendered by the hierarchical structure have fostered the development of novel bioinspired materials. However, the stochastic aspects have received little attention. Here, we first review our recently proposed fishnet statistical model for nacreous biomimetic materials [6–9] (as presented at the Century Fracture Mechanics Summit in Singapore on April 8, 2019). Then, we extend this model to architected nanomaterials and show that it may also capture some failure probability features of quasibrittle materials in general, including concrete or fiber composites.

Traditionally, only two major analytically tractable models for strength statistics have been available—the weakest-link chain (or the series coupling model due to Weibull [10]) and the fiber bundle (or the parallel coupling model due to Daniels [11]). Based on the power-law form of the failure probability tail, which is justified by the extreme value theorem [12], and according to Refs. [13,14], also by the statistics of interatomic bond failures, the weakest-link model leads to the Weibull distribution, while the strength of a fiber bundle follows the Gaussian (or normal) distribution [11].

Furthermore, it has been shown that, to capture quasibrittleness and the plastic-brittle transition of size effect, the number of links in the weakest-link model must be finite and depend on the structure size [13–19]. This concept has recently been extended for the strength distribution of MEMS devises [20]. The lower tail of the strength distribution of fiber bundles with a general fiber softening constitutive law has been clarified by Salviato and Bažant [21].

Both the weakest link and fiber bundle models are idealizations of the internal material failure mechanism, representing simplified internal connectivity and force transmission. These simplifications enable the mathematical formulations of their strength probability distribution. Recently [6–8], the force transmission in nacreous

[1]Corresponding author.

Contributed by the Applied Mechanics Division of ASME for publication in the Journal of Applied Mechanics. Manuscript received November 2, 2019; final manuscript received November 26, 2019; published online December 4, 2019. Assoc. Editor: Yonggang Huang.

materials has been idealized as a fishnet with brittle links pulled diagonally, which allowed a mathematical formulation of the fishnet statistics. The fishnet represents the third probabilistic model of strength distribution that is tractable analytically.

Unlike a single chain, whose failure and maximum load are triggered by the rupture of a single link, the weakest one, a fishnet, possesses multiple structural redundancies. Before reaching the maximum load, the fishnet may already contain several failed links, whose number generally increases with the coefficient of variation on link strength scatter. To capture it, the fishnet statistical model splits the fishnet survival event into a union of disjoint events corresponding to different numbers of failed links at the prescribed load σ. Thus, the failure probability of fishnet gets reduced to a series of powers of the distribution, $P_1(\sigma)$, of link strength.

This formulation works well for brittle nacreous materials, because the failed links at the peak load are not that many. A few terms in the series expansion suffice for a good approximation of the distribution. In this sense, the fishnet model series expansion can be seen as a perturbation of the weakest-link model. On the other hand, it is relatively hard to extend the expansion method to quasibrittle materials, whose links exhibit progressive postpeak softening of various steepness. As the links become less brittle, more widely scattered damages occur before the peak load. So, more higher-order terms have to be considered. It is, however, very tedious to calculate them and their expressions vary for different geometry and loading conditions. Therefore, another approach is needed for fishnets with softening links.

In Ref. [8], it was shown that the strength distribution of a fishnet with gradually softening links can be well approximated by order statistics. It is no longer necessary to consider the weakest of the remaining links. Rather it suffices to consider the kth weakest link that determines the peak load of the whole structure. The order k reflects the extent of damages right before the maximum load, with k being in itself a discrete random variable. The probability mass function (pmf) of the order is approximated using the geometric Poisson distribution (also called Pólya–Aeppli distribution), which accounts for the random cluster nature of the damages.

Here, we show that the series expansion and the theory based on order statistics are actually equivalent—both of them are power series of the link strength distribution $P_1(\sigma)$. Then, we propose a general expression for the fishnet probabilistic model based on this observation. The fishnet model demonstrates the potential of significantly reducing the failure risk of a material by carefully designing its microstructure such as the distinctive "brick-and-mortar" structure of nacre.

Recently, it has been shown that a thin film of cellulose nanocrystal has a statistical size effect similar to fishnet's [22], implying that the fishnet model may apply to this type of material. Thanks to the general formulation of the fishnet probabilistic model, we can apply it at the low probability tail to quasibrittle particulate materials such as concrete, to fiber composites, and to architected nanomaterials such as the octet-truss nanolattice.

First introduced by Fuller [23], deterministic modeling of the octet-truss lattice system has been pursued intensively due to its high stiffness-to-mass ratio and excellent energy absorption capability [24,25]. Therefore, it has long been perceived as an alternative to replace foams and honeycombs in lightweight structures. With the advent of 3D printing, the manufacturing of octet-truss nanolattice became easier.

In a deterministic manner, the octet-truss properties have been studied both numerically and analytically [26–28]. However, the reliability and probability distribution of the nanostructure strength, which have not been studied yet, will become increasingly important. More nano-architected materials will doubtlessly appear in engineering applications.

The Weibull statistics is the large-size asymptotics of the type 1 energetic-statistical size effect [15,16]. The energetic release part, dominant for small sizes, has been explained by stress redistributions due to a large fracture process zone (FPZ) and can be regarded as the limit case of the energetic size effect, type 2, for vanishing initial stress-free crack. The fishnet statistics, on the other hand, can be regarded as a modification, or generalization, of the type 1 size effect law, in which the energy release aspect is reflected in the interaction of multiple link breaks prior to reaching the maximum load.

2 Review of the Fishnet Statistics

2.1 Fishnet Statistics With Series Expansion. Nacre, well known for its astonishing strength, has a staggered "brick-and-mortar" micro-structure (see Fig. 1(*a*)), in which the "bricks," about 400 nm in thickness, are strong platelets of aragonite (a polymorph of calcium carbonate, or calcite, $CaCO_3$, with an orthorhombic crystal system). The "mortar" is a bonding layer of compliant bio-polymer, <10 nm in thickness. As proposed in Refs. [6,7], the staggered micro-structure of nacre is, for statistical purposes, best idealized as a fishnet (Fig. 1(*b*)) consisting of brittle links pulled diagonally.

For calculations, we consider here a two-dimensional (2D) fishnet consisting of n rows and m columns of links ($N = m \times n$), whose strengths are independent and identically distributed (i.i.d.) random variables. Their probability distribution $P_1(\sigma)$ is assumed to be a grafted Gauss–Weibull distribution [15,29] having a Weibull (or power-law) lower tail.

Let $P_f(\sigma)$ be the fishnet probability of fishnet under load (or average stress) σ applied at boundary. Unlike a single chain, more than one link may fail prior to reaching the peak load of the whole fishnet. We therefore extend the weakest-link model and seek the expression of survival probability $1 - P_f$ in the form of a series expansion

$$1 - P_f(\sigma) = P_{S_0}(\sigma) + P_{S_1}(\sigma) + P_{S_2}(\sigma) + \cdots \tag{1}$$

where $P_{S_k}(\sigma)$ is the probability that the whole fishnet survives under load σ when there are exactly k failed links. Clearly, the first term $P_{S_0}(\sigma)$ in the above expansion is the same as the weakest-link model and equal to $[1 - P_1(\sigma)]^N$. The remaining terms, $P_{S_k}(\sigma)$, are what makes the fishnet model distinct from the weakest-link model. The terms are summed because it represents a union of disjoint (mutually exclusive) event. The second term is

$$P_{S_1}(\sigma) \simeq NP_1(\sigma)[1 - P_1(\sigma)]^{N-\nu-1}[1 - P_1(\eta\sigma)]^{\nu} \tag{2}$$

where $\eta\sigma$ is the equivalent redistributed stress in the fishnet caused by prior link failure [7] and ν is the number of links near the failed one that undergo significant stress redistribution. Equation (2) is derived as the joint probability of failure of one of the N links occurring jointly with the survival of all the remaining links.

The analytical expression for $P_{S2}(\sigma)$ is more complicated; see Eqs. (9)–(12) in Ref. [6]. For the higher terms, the analytical expressions become prohibitively complicated but are not needed since millions of Monte Carlo simulations showed that the first three terms are normally close enough to the exact solution (except for unusually large coefficients of variation of link strength).

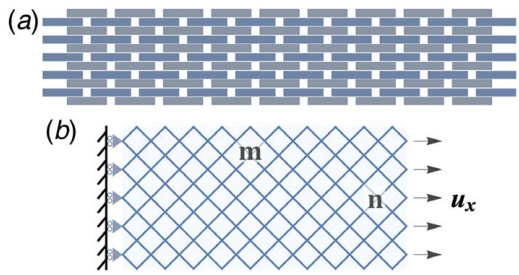

Fig. 1 (*a*) Schematic showing the micro-structure of nacre and (*b*) fishnet structure simplified from nacreous connectivity

If we keep only the first term P_{S_0} on the right-hand side of Eq. (1), discarding the other terms, we have the classical weakest-link model, i.e.,

$$1 - P_f(\sigma) = P_{S_0}(\sigma) = [1 - P_1(\sigma)]^n \tag{3}$$

Because of all the terms in Eq. (1) are non-negative, the weakest-link model shown in Eq. (3) (as well as its limiting Weibull distribution) is an upper bound on the true failure probability of the fishnet. To compare the two models, we convert the expressions of failure probability P_f into the Weibull scale, where the x coordinate is transformed from σ to $\ln \sigma$ and the y coordinate is transformed from P_f to $\ln[-\ln(1-P_f)]$. Weibull distributions become straight lines under this transformation, which makes it easier to see the difference between the weakest-link and fishnet models.

The Taylor series expansion shows that the second term $P_{S_1}(\sigma)$ causes the slope of P_f to increase by a factor of two at the lower tail. This makes the structure significantly safer at the 10^{-6} failure probability level. Figure 2 compares the finite weakest-link model and the 2-term fishnet model. The upper tail ($P_f \geq 0.01$) for both models is almost the same, while the slope of the curve has doubled at the lower tail ($P_f \leq 10^{-5}$) of the 2-term fishnet model, leading to a higher strength at $P_f = 10^{-6}$ and a much lower failure probability under the same stress.

The third term in the series, whose leading-order term is $P_1(\sigma)^2$, can be formulated in a similar fashion. This leads, in the Weibull scale, to a lower tail asymptote with a triple of the Weibull slope. However, due to accumulation of error in using the effective, rather than exact, redistributed stress, the higher-order terms become less accurate. This is not a big issue for most brittle materials, since for them the series converges very fast and only two to three terms are needed, and the asymptotes of higher-order are approached only for P_f much less than 10^{-6}.

Note that, at the lower tail, the general form of the survival probability, Eq. (1), can be rewritten as a power series of $P_1(\sigma)$:

$$1 - P_f(\sigma) = a_0 + a_1 P_1(\sigma) + a_2 P_1(\sigma)^2 + a_3 P_1(\sigma)^3 + \cdots \tag{4}$$

For instance, $a_0 = P_{S_0} = [1 - P_1(\sigma)]^N \sim 1$ and $a_1 = P_{S_1}/P_1 \simeq N[1 - P_1(\sigma)]^{N-\nu-1}[1 - P_1(\eta\sigma)]^{\nu} \sim N$. This is because, for each survival probability, $P_{S_k}(\sigma)$ is the product of the failure probabilities of k individual links with the jointly occurring survival probabilities of the remaining $N-k$ links.

At the lower tail, the survival probabilities all tend to 1. So, the failure probabilities dominate at the tail, and they all come in the form of $P_1(\sigma)^k$.

2.2 Fishnet Model With Order Statistics. The link damages tend to be more dispersed in fishnets whose links are less brittle, and so more higher order terms are needed to determine the effect of decreasing link brittleness on the overall structure failure probability. To model the strength distribution of more general quasibrittle biomimetic materials, we have previously introduced order statistics into our fishnet model [8]. The main purpose was to overcome the difficulty in capturing the stress redistribution history around link damages for the higher-order terms of the series expansion. If the decrease of link force from the peak to zero is decomposed into k downward jumps, and if k is not too small, the stress redistribution due to each jump becomes negligible. This is the advantage of turning to order statistics.

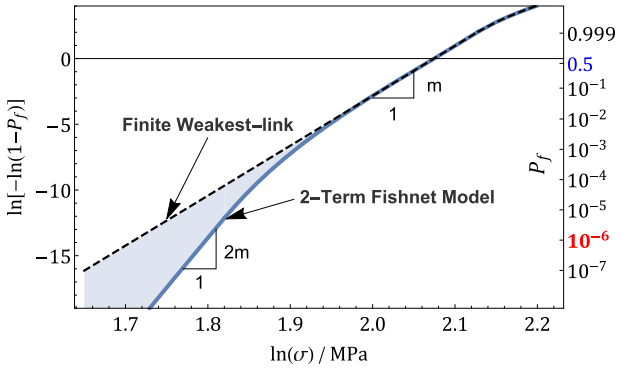

Fig. 2 Comparison of the 2-term fishnet model and the finite weakest-link model under the Weibull scale for an 8 × 16 brittle fishnet

The strength distribution of the kth smallest minimum (kth order statistic) is used to approximate the nominal strength of the whole structure under uniaxial tension, given that the kth damage gives the peak load, triggering failure. Then, the order statistics distributions form a family of bases whose linear combination gives the failure probability:

$$P_f(\sigma) = \mathbb{P}(\sigma_{\max} \leq \sigma) = \sum_{k=0}^{N} \mathbb{P}(N_c = k) W_k(\gamma_k \sigma) \tag{5}$$

where N_c is the number of link damages right before the peak load is reached, $W_k(x)$ is the cumulative distribution function of the distribution of the kth strength order statistics, and γ_k is the average stress concentration factor for various k values. Since $W_k(x)$ alone is only an approximation of the peak load, γ_k is introduced as a corrector that depends on the mean behavior of the stress redistribution, which is implicitly affected by the brittleness of the material. The expression of $W_k(x)$ is known to be [8]

$$W_k(x) = 1 - [1 - P_1(x)]^N \sum_{s=0}^{k} \frac{\{-N \ln [1 - P_1(x)]\}^s}{s!} \tag{6}$$

Because the damages tend to cluster, $\mathbb{P}(N_c = k)$ is properly modeled by the geometric-Poisson distribution [30]

$$\mathbb{P}(N_c = k) = \begin{cases} \displaystyle\sum_{s=1}^{k} e^{-\lambda} \frac{\lambda}{s!} \binom{k-1}{s-1} \theta^s (1-\theta)^{k-s}, & k = 1, 2, 3, \ldots \\ e^{-\lambda}, & k = 0 \end{cases} \tag{7}$$

where λ and θ are two empirical parameters that need to be calibrated by test data.

3 General Form of the Strength Distribution in Fishnet Statistics

Up to now, we have considered two different approaches to obtain P_f in the fishnet model. In this section, we show that the two approaches are actually consistent. In other words, the fishnet model with order statistics can be written in the form of power series expansion in terms of $P_1(\sigma)$. $P_1(\sigma) \sim (\sigma/\sigma_0)^m$ at the lower tail. Based on Eq. (6), the expression of P_f using order statistics is

$$P_f(\sigma) = \sum_{k=0}^{N} c_k W_k(\gamma_k \sigma) = 1 - \sum_{k=0}^{N} c_k (1 - P_1(\gamma_k \sigma))^N \times \sum_{s=0}^{k} \frac{(-N \ln(1 - P_1(\gamma_k \sigma)))^s}{s!} \tag{8}$$

Let N be sufficiently large. Then, $(1 - P_1(\sigma))^N$ tends to the Weibull distribution, i.e., to $e^{-N(\sigma/\sigma_0)^m}$, where $P_1 \sim (\sigma/\sigma_0)^m$. For simplicity, let $x = \sigma/\sigma_0$. Substitution into the foregoing expression yields

$$1 - P_f(x) = c_0 e^{-N(\gamma_0 x)^m} \cdot 1 \tag{9}$$

$$+c_1 e^{-N(\gamma_1 x)^m}\cdot\left[1+\gamma_1^m N x^m\right] \tag{10}$$

$$+c_2 e^{-N(\gamma_2 x)^m}\cdot\left[1+\gamma_2^m N x^m+\gamma_2^{2m}\frac{(Nx^m)^2}{2!}\right] \tag{11}$$

$$+c_3 e^{-N(\gamma_3 x)^m}\cdot\left[1+\gamma_3^m N x^m+\gamma_3^{2m}\frac{(Nx^m)^2}{2!}+\gamma_3^{3m}\frac{(Nx^m)^3}{3!}\right] \tag{12}$$

$$+c_4 e^{-N(\gamma_4 x)^m}\cdot\left[1+\gamma_4^m N x^m+\gamma_4^{2m}\frac{(Nx^m)^2}{2!}+\gamma_4^{3m}\frac{(Nx^m)^3}{3!}+\gamma_4^{4m}\frac{(Nx^m)^4}{4!}\right] \tag{13}$$

$$+\cdots \tag{14}$$

After the Taylor series expansion of $e^{-N(\gamma_k x)^m}$ in the foregoing expression, Eq. (8) can be rewritten in the form of Eq. (4). A unique correspondence between the coefficients a_k, γ_k and c_k can then be obtained by equating the two expressions.

Furthermore, it can be shown, via Taylor series expansion, that the distribution of the kth order statistics has the leading term of $(\sigma/\sigma_0)^{km}$. Therefore, its lower tail in the Weibull-scale plot has slope km. In other words, the slope of P_f at its lower tail is fully controlled by the first non-zero coefficient c_k.

Noting that γ_k is very close to 1 in general (e.g., 1.04), we could, for simplicity, replace γ_k for various k values by their average, γ. Then, the survival probability reduces to a neat expression

$$1-P_f(\sigma)=e^{-N(\gamma x)^m}\cdot\left[f(0)+f'(0)N\gamma^m x^m+f''(0)\frac{(N\gamma^m x^m)^2}{2!}+f'''(0)\frac{(N\gamma^m x^m)^3}{3!}+f^{(4)}(0)\frac{(N\gamma^m x^m)^4}{4!}+\cdots\right] \tag{15}$$

or

$$\boxed{P_f(\sigma)=1-e^{-N\gamma^m x^m}\cdot f(N\gamma^m x^m)} \tag{16}$$

where

$$f(0)=1 \tag{17}$$

$$f'(0)=1-c_0 \tag{18}$$

$$f''(0)=1-(c_0+c_1) \tag{19}$$

$$f'''(0)=1-(c_0+c_1+c_2) \tag{20}$$

$$\cdots \tag{21}$$

$$f^{(k)}(0)=1-\sum_{i=0}^{k-1}c_i \tag{22}$$

The expression in the brackets of Eq. (15) can be seen as a Taylor series expansion of some function $f(y)$ about $y=0$, where $y=N\gamma^m x^m$. The sequence of derivatives $\{f^{(k)}(0)\}$, strictly decreasing from 1 to 0, is the complementary cumulative distribution function of the damage extent N_c. In this sense, f is determined purely by the stress redistribution process, which in turn depends on the mechanical properties of the material.

Thus, the determination of P_f gets reduced to the characterization of the function f or, equivalently, of its derivatives at 0. In the special case of the weakest-link model, function f is simply a constant equal to 1, and P_f then reduces to the Weibull distribution.

4 Application of Fishnet Statistics to Quasibrittle Materials in General

4.1 Tensile Strength Distribution of Octet-Truss Nanolattice. A careful look at the octet-truss lattice structure reveals that it is actually a union of three systems of parallel fishnets aligned in three orthogonal directions. From Fig. 3, it is clear that the three families of parallel fishnets lie in xy, yx and xz planes. Because the lattice consists of fishnets in three directions, the connectivity (or nodal coordination number) at each node is three times larger than that of the fishnet. This greatly enhances the redundancy of the microstructure, positioning the octet-truss tail farther away from the brittle weakest-link tail and closer to the ductile fiber-bundle tail. Therefore, compared to a single 2D fishnet, we expect a huge safety gain of the octet-truss structure at the lower tail of the strength distribution.

Here, we model the strength distribution of an $8\times4\times4$ octet-truss nanolattice, as shown in Fig. 4. Many materials have been used to print the lattice structure on the meso- or nano-scale, e.g., pyrolytic carbon [26] and copper [27,28]. With no loss of generality, we take the properties of the nanolattice truss links to be of the same magnitudes as reported in the literature (see Table 1). To model the gradual failure process, a finite element (FE) code with an infinitesimal strain measure is developed in c++ using Eigen 3.3.7 [31] linear algebra library. The visualization of the results is conducted in Paraview 5.7 [32]. Instead of using the encastre boundary conditions on one end, the nodes on the outer faces of the yz, xz and xy planes with outward normals $(-1, 0, 0)$, $(0, -1, 0)$ and $(0, 0, -1)$ are subjected to boundary conditions $u_x=0$, $u_y=0$ and $u_z=0$, respectively. This is to guarantee that every middle cross-section undergoes the same contraction. Then, uniaxial tension is applied by prescribing the horizontal displacements u_x of the nodes on the outer face with outward normal (1, 0, 0). The remaining two boundaries are considered as free surfaces with no external load.

The strengths of the truss elements (or links) are randomized based on a grafted Gauss–Weibull distribution [13], which has a Weibull lower tail $P_1(\sigma)=1-\exp[-(\sigma/100)^{10}]$, and on a Gaussian distribution, $\mathbf{N}(100, 16^2)$ for the rest. The current settings of mean

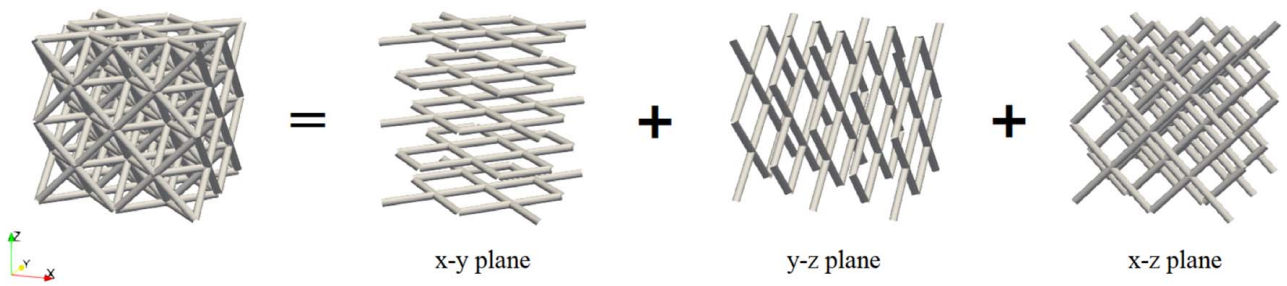

Fig. 3 Octet-truss nanolattice can be seen as the union of fishnets aligned in three orthogonal directions. Each fishnet node on its inside has connectivity 4, while each node inside of an octet-truss nanolattice has connectivity 12.

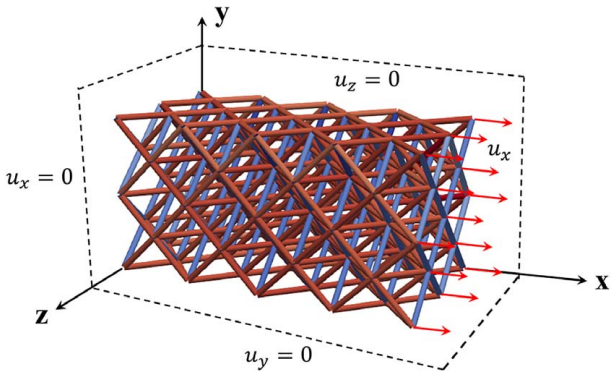

Fig. 4 Loading and boundary conditions for the 8 × 4 × 4 nanolattice in finite element simulation

Table 1 Truss properties

Young's modulus	Mean strength	Length	Cross-sectional diameter
10 GPa	≃100 MPa	2 μm	0.5 μm

strength and element stiffness guarantees that the failure strains of the links are very small, and so our assumption of a linearized infinitesimal strain measure holds. The grafting point is set at $P_f = 10^{-3}$ (as in Ref. [8]). The truss links are here considered brittle; i.e., once the strength limit of a link (or truss element) is reached, its stress immediately drops to 0.

In each simulation, the structure is first loaded by a trial displacement u_0, then the ratio of strength over stress is calculated for each link. The minimum ratio is the smallest load multiplier that will cause one and only one link failure in the whole structure. Next, all the variables are updated by the smallest multiplier, according to the linear elasticity of the structure. Then, the critical element is deleted by removing its contribution from the global stiffness matrix. Finally, the damaged structure is treated as a new one and is loaded again from origin by the trial displacement u_0. This process is repeated until complete failure. In other words, the driving parameter for the simulation is the number of failed links in the truss system, while displacement control is used within each step. In these simulations, we suppress compression failures of the truss links by assigning them very large strength. The links under compression are those in the yz plane. They are under compression from the beginning and are excluded from our probabilistic modeling.

One million Monte Carlo simulations have been conducted using a FE code. Figure 5 shows the load–displacement curves of 1000 samples. The peak loads are marked by solid points. Since the

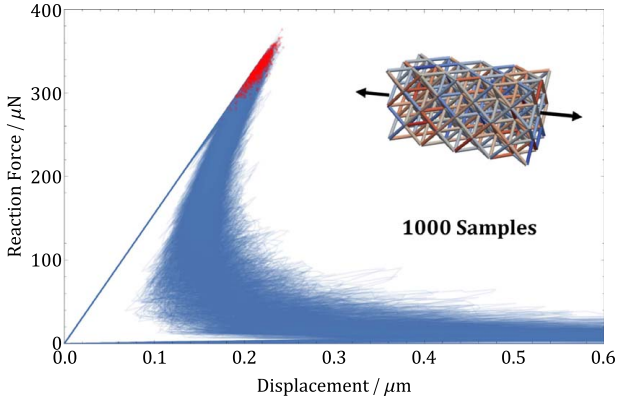

Fig. 5 Load–displacement curves for 1000 Monte Carlo simulations. Maximum loads are marked by solid points

truss elements are treated as brittle, the load–displacement curves exhibit snap-back instability in the post-peak regime. If the maximum load is reached right before the failure of the weakest link, the peak load point will be on the line of initial stiffness (or slope) of the load–displacement curve. Otherwise, the peak load point will lie underneath the line of initial stiffness. As is clear from Fig. 5, most of the peak loads lie slightly off the initial stiffness line, which indicates that they happen after a few links have failed. Only a small portion of peak loads are triggered by the first failure of links. This is beneficial for safety and occurs, thanks to the redundancies in the octet-truss connectivity.

Before modeling the strength distribution of the octet-truss nanolattice, we must define the nominal stress, σ. We do so as follows:

$$\sigma = c_n \frac{P}{A} \tag{23}$$

where P is the total reaction force from the cross-section, A is the cross-sectional area of the octet-truss lattice, and c_n is a normalizing constant to convert the average stress in a cross section to the stress in a tensile member. For the current octet-truss nanolattice, its cross-sectional area is $A = 13 \times \pi d^2/4 = 2.553\ \mu\text{m}^2$ and $c_n = 0.4784$.

For the analytical strength distribution, we evaluate and compare several existing models: (1) weakest-link model, (2) 2-term fishnet model, (3) 3-term fishnet model, (4) the general fishnet distribution (Eq. (16)), and (5) the fiber-bundle model. Evaluating the weakest-link model is straightforward

$$P_f(\sigma) = 1 - [1 - P_1(\sigma)]^N \tag{24}$$

where $N = 320$ is the number of members in tension under the initial loading. The elements in the yz plane are under compression and are not counted. Then, the 2-term fishnet model can be evaluated on the basis of the weakest-link model by adding the probability that the whole fishnet remains safe under σ with one and only one failed link:

$$P_f(\sigma) = 1 - [1 - P_1(\sigma)]^N - NP_1(\sigma)[1 - P_1(\sigma)]^{N-\nu-1}[1 - P_1(\eta\sigma)]^\nu \tag{25}$$

where $\eta = 1.15$; $\nu = 5$ gives the best fit. Again, the 3-term fishnet model can be formulated on the basis of the 2-term fishnet model [7]

$$P_f(\sigma) = 1 - [1 - P_1(\sigma)]^N - NP_1(\sigma)[1 - P_1(\sigma)]^{N-\nu-1}[1 - P_1(\eta\sigma)]^\nu \tag{26}$$

$$-N\nu_1[1 - P_1(\sigma)]^{N-\nu_2-2}\,[1 - P_1(\eta^{(2)}\sigma)]^{\nu_2} \int_0^{\sigma} \int_{x_1}^{\eta_b^{(1)}\sigma} \psi(x_1)\psi(x_2)\,dx_2\,dx_1 \tag{27}$$

$$-N(N - \nu_1 - 1)[1 - P_1(\sigma)]^{N-2\nu_1-2}[1 - P_1(\eta^{(2)}\sigma)]^{2\nu_1} \times \int_0^{\sigma} \int_{x_1}^{\sigma} \psi(x_1)\psi(x_2)\,dx_2\,dx_1 \tag{28}$$

where $\psi(\sigma) = P_1'(\sigma)$ is the probability density for the link strength, $\nu_1 = 8$, $\nu_2 = 18$, $\eta^{(2)} = 1.5$, and $\eta_b^{(1)} = 1.115$.

As can be seen from the previous formulations, the expression of the failure probability becomes increasingly complicated as we keep adding more survival probabilities. It will be much easier to use the general expression of the fishnet model (Eq. (16)), if many higher order terms should be considered.

The key step is to characterize the unknown decreasing function f (or its derivatives at 0) in the expression (Eq. (16)). The optimum fit using this expression can be achieved by setting $\gamma = 1.075$ and $f(0) = f'(0) = f''(0) = \cdots = f^{(4)}(0) = 1$. The remaining higher-order derivatives remain 0. In other words, it is simply the distribution of the fifth-order statistic of link strengths.

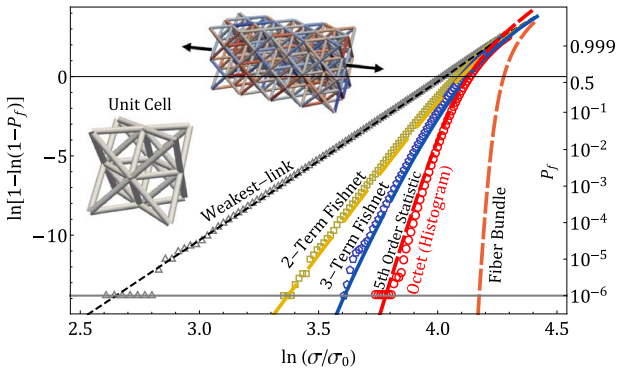

Fig. 6 Strength histogram (shown in circles) of the strength of octet-truss nanolattices under the Weibull scale compared with different analytical models. The sample size is 10^6.

Finally, for the fiber bundle model [11], the limiting distribution is a Gaussian (normal) distribution with mean $=\tau[1-P_1(\tau)]$ and standard deviation $=\tau\sqrt{P_1(\tau)[1-P_1(\tau)]/n}$, where τ is the value of x such that the average stress–strain curve, $xP_1(x)$, takes its maximum value.

Figure 6 shows the strength histogram (shown by circle points) of the octet-truss nanolattice together with various analytical probabilistic models of material strength, as mentioned above. Also shown in the figure are the computed histograms of (1) the load at the first step (first link failure) (triangles), (2) the maximum load of the first two steps (squares), and (3) the maximum load of the first three steps (pentagons). Since the sample size of our Monte Carlo simulations is 10^6, the histograms have reached $P_f=10^{-6}$ probability level and have converged at about $P_f=10^{-5}$.

It is clear that the general expression of the fishnet model, Eq. (16), gives, for the distribution of fifth-order statistic, the closest match of the computed histogram, except at the upper tail. This is because we used a single γ to replace the different values of γ_k for various k values. The weakest-link model, the 2-term and 3-term fishnet models are upper bounds on the actual strength distribution. They match very well the histogram of the maximum loads of the first two and three steps, respectively. It is clear that, as we add more terms in Eq. (1) for the survival probability, the distribution gradually approaches the histogram. Also note that the Gaussian distribution for the fiber bundle gives a lower bound.

At the extremely low probability level of $P_f=10^{-6}$, the 2-term fishnet model gives a nominal strength that is 92% higher than the weakest-link model does. Comparing the 2-term and 3-term fishnet models, the 3-term fishnet model predicts a further 27% strength increase. The actual histogram and the distribution of the 5th-order statistic indicate an additional 18.5% nominal strength increase relative to that of the 3-term fishnet model at the $P_f=10^{-6}$ tail. However, at the median level (i.e., for $P_f=0.5$), the strength values given by these models are very close. The median strength increase is merely 12% between the weakest-link model to the distribution of the 5th order statistic. But the 10^{-6} quantile has a 209% increase, which is enormous.

It thus becomes clear that paying attention only to the mean strength of a material does not suffice to optimize material or structure design. It does not guarantee robustness and reliability. The connectivity of the microstructure does play a determining role in the tail strength of a material. A smart design of such connectivity, as in the case of octet-truss nanolattice, makes a huge difference for optimizing a printed material microstructure.

Within the range of brittle materials, the brittle fiber bundle gives the lowest possible failure probability for each prescribed load and the highest possible strength at all probability levels. It is the theoretical limit of architected material strength. But there is a serious limitation for the fiber bundle—it can carry load in only one direction.

The 3D lattices, on the other hand, can carry multiple loads in different directions. In this sense, although the octet-truss nanolattice is not as reliable as the fiber bundle under loads of a single orientation, in terms of overall reliability, for loads of different orientations it surpasses the fiber bundle.

To sum up, there are always trade-offs in material performance under loads of different orientations.

4.2 Tensile Strength Distribution of Concrete and Composites in General. A homogeneous specimen (or structure) of a brittle material with a negligible material strength variability and a negligible FPZ compared to specimen dimensions fails as soon as a crack begins to grow, provided that the structure geometry is positive (which means a geometry for which the derivative of energy release rate with respect to the crack length at constant load is positive). Obviously, the strength must then follow the weakest-link model exactly. However, for quasibrittle materials, there are deviations. The Gauss–Weibull distribution was shown to capture them [13–15], but not necessarily for the extreme lower tail in the 10^{-6} range.

Recent simulations of the tensile force transmission chains in a concrete prism loaded in tension [33] reveal a combination of axial and inclined interparticle forces. The inclined ones represent lateral interactions and suggest a partial fishnet action to be present. This is certainly a possibility since no existing histogram data give information below $P_f=0.01$. The same is probably true of all quasibrittle materials, including coarse-grain ceramics, granular rocks, sea ice, wood and fiber composites, especially textile composites.

4.2.1 Correction of Weibull's Histogram Plots of Test Data for Concrete. Let us now consider concrete. The earliest, and still the most extensive, test data on the distribution of the tensile strength of concrete can be found in Weibull's paper in 1939 [10]. He tested three batches of specimens with reduced-size aggregate, cured in water for 2, 7, and 28 days. The statistical sample sizes were 680, 1082, and 1106, respectively. The whole histogram testing took about one year to finish. The original unit used for stresses and strengths in Weibull's paper was kg/cm^2 (which equals 0.098067 MPa and kg here means kilogram-force). We keep here this unit in discussing his tests. We now explore the possibility of using our fishnet model to fit these original test data and discuss the strength predicted at 10^{-6} probability level.

For each data set for various materials presented in Weibull's paper, he or his assistant fitted the measured histograms using either 2-parameter or 3-parameter Weibull distribution, whichever fitted the best. For the tensile strengths of concrete, they chose the 3-parameter Weibull distribution because the histogram was not a straight line in the 2-parameter Weibull scale. But in 2007, it was shown [13], based on the probability of interatomic bond breaks, that a finite threshold used in the 3-parameter Weibull distribution is, for material strength distribution, physically unjustifiable (since it conflicts with Kramer's rule of transition rate theory for statistics of interatomic bond breaks, whose validity is beyond doubt). Therefore, as in [13], we convert Weibull's test data from the 3-parameter Weibull scale to the 2-parameter Weibull scale.

It was during this data conversion process that we uncovered an inconsistency (apparently enduring since 1939) in the types of logarithm used for the vertical and horizontal axes, as presented in Weibull's original paper [10]. For the horizontal (log-strength) axis, his assistant who did the data fitting must have used the common (or decadic, Briggs') logarithm (of base 10) or else the model parameters presented in Weibull's paper would not match the data, while for the vertical axis, he or she must have used the natural logarithm (base e), because assuming the common logarithm would lead to wholly unreasonable tail probabilities for the test data. Therefore, we converted all Weibull's data to the 2-parameter Weibull scale using the natural logarithm.

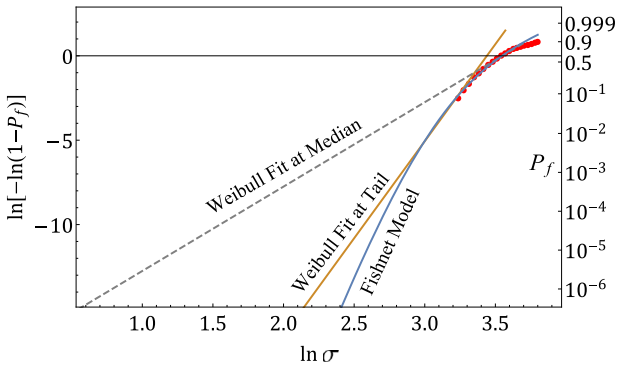

Fig. 7 Fitting of the Weibull's 1939 histogram test data on the tensile strength of concrete (seven days in water) by 2-parameter Weibull distribution and fishnet model

4.2.2 Analysis of Corrected Plots of Weibull's Histograms. The solid points in Fig. 7 show the histogram data of Weibull's original tests on concrete specimens converted into 2-parameter Weibull scale: $X = \ln\sigma$ and $Y = \ln(-\ln(1-P_f(\sigma)))$. Although his sample size for concrete was 1082, the data points in Weibull's histogram plots reach only $P_f = 0.1$ and $P_f = 0.9$ for the lower and upper tails, respectively. This is because, before plotting the data, Weibull first grouped the data into bins, each aggregating about 1–10 points, which greatly decreased the histogram scatter but reduced the sample size (i.e., the number of data points). In contrast to the 3-parameter Weibull plot, the test data under the 2-parameter Weibull scale can no longer be fitted well by a straight line (as explained in [13]).

Also shown in Fig. 7 are the optimum fits of the test data by various statistical models. The optimal number of links for the fishnet statistics is $n = 100$. It is clear that the tangent (Weibull distribution) through the median section gives a much more conservative prediction than the tangent through lower tail, and even more conservative compared to the fishnet model.

The fishnet model prediction indicates a further slope increase of the curve at its lower tail, leading to a 5.13% tail strength increase compared to the Weibull distribution fit at data tail. This extra safety gain can be explained only by the redundancy of the force chain for concrete under uniaxial loading. The pattern of the force chain was simulated by Nitka and Tejchman [33] using the discrete element method.

Though not the same, the force chain pattern is similar to that of a fishnet. A histogram test with a much larger sample size would help to clarify which model of the two gives a more realistic prediction at the extreme lower tail. A better check could result from the analysis of size effect.

5 Conclusions

(1) The fishnet model with a series expansion of survival probabilities for brittle nacreous material is equivalent to the recent formulation with order statistics for fishnets with links of arbitrary softening slopes. Both of them can be written in the form of a power series in terms of the link strength distribution.
(2) A unified general formula for the fishnet probabilistic model is possible and its mathematical form has been proposed.
(3) The fishnet model is applicable to the strength distribution of octet-truss nanolattices. Their nodal connectivity, which is three times as large as–that of the 2D fishnet, results into more extensive and more uniform stress redistribution after a link fails. This leads to a major safety gain at the risk level of one out of a million.
(4) Millions of Monte Carlo simulations of the failure of the octet-truss nanolattice confirm the analytical results.
(5) The fishnet model has been used to fit the original Weibull's test data on the strength distribution of concrete. The prediction of strength at 10^{-6} probability level shows a small increase compared to that given by the Weibull distribution fit of the histogram lower tail. It indicates that the force chain connectivity in concrete could also provide some structural redundancy, though not as much as in nacre.
(6) Unnoticed since 1939, Weibull's original plot of his test data utilized different and mutually incompatible types of logarithms for the horizontal and vertical axes. From now on, the present correction should be used.

Acknowledgment

Financial support under ARO Grant W91INF-19-1-0039 to Northwestern University is gratefully acknowledged. Thanks are due to professor Jia-Liang Le of University of Minnesota and professor Sze Dai Pang of National University of Singapore for valuable discussions.

Appendix

Further explanation is in order on the original paper published in 1939 [10], in which Weibull did not mention exactly which type of logarithm he had used for plotting the data. Here, we show that in the original plot of the test data on concrete, Weibull or his assistant adopted the common logarithm (Briggs', base 10) for the x-axis, $X = \log_{10}(\sigma - \sigma_u)$, and the natural logarithm (base e) for the y-axis, $Y = \ln[-\ln(1-P_f)]$.

First, we focus on the y-axis. Figure 8 shows the Weibull's original test data plotted under two different log scales. The ticks on the left use the common logarithm with base 10. It can be easily seen that the data range from $P_f \simeq 0.01$ up to $P_f \simeq 0.99999$. The lower and upper limits are highly unsymmetrical. In addition, it is almost impossible for the test data to reach the range of $P_f = 0.99999$, since that would require at least 10^5 repetitions of the same test. In this paper, Weibull indicated that there were only 1082 samples tested. Therefore, it does not make sense to assume that common logarithm is used for the y-axis. On the other hand, if we try to mark the ticks by natural logarithm (shown on the right of the figure), the data look much more reasonable. It now ranges from $P_f \simeq 0.1$ to $P_f \simeq 0.9$, which is symmetric.

Furthermore, because Weibull mentioned in the paper that he grouped the data into small bins, it makes the actual sample size much smaller. This explains why the plotted data did not reach 0.001 and 0.999 probability levels for the lower and upper limits, respectively. From the practical point of view, the analytical expression of Weibull distribution always contains a natural log base e, so it would be inconvenient to use the common logarithm when converting the distribution function to the Weibull scale.

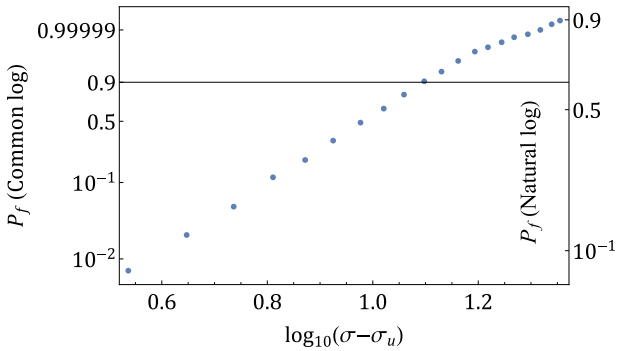

Fig. 8 Replot of Weibull's 1939 test data (seven days in water) using two different logarithms. Ticks on the left use common logarithm and those on the right use natural logarithm.

Next, we switch our focus to the horizontal axis. Weibull used the 3-parameter Weibull distribution to fit the data

$$P_f = 1 - e^{-[(\sigma-\sigma_u)/\sigma_0]^m} \tag{A1}$$

where σ_u is the finite threshold, m is the Weibull modulus, and σ_0 is the scale parameter. The reported values for the fitting parameters are $\sigma_u = 22$ kg/cm^2, $m = 4.6$, and $\sigma_0 = 12.6$ kg/cm^2. The easiest way to figure out which type of logarithm is used is to check the x-intercept of the data. If the common logarithm were used, the straight line equation in Weibull scale would have been

$$\log_{10}[-\log_{10}(1-P_f)] = m\log_{10}(\sigma-\sigma_u) - m\log_{10}\sigma_0 + \log_{10}(\log_{10} e) \tag{A2}$$

where $X = \log_{10}(\sigma-\sigma_u)$ and $Y = \log_{10}[-\log_{10}(1-P_f)]$. The resulting x-intercept would have been

$$X_0 = \log_{10}\sigma_0 - \frac{1}{m}\log_{10}(\log_{10} e) \tag{A3}$$

But if the natural logarithm is used, the equation for the straight line under Weibull scale becomes

$$\ln[-\ln(1-P_f)] = m\ln(\sigma-\sigma_u) - m\ln\sigma_0 \tag{A4}$$

where $X = \ln(\sigma-\sigma_u)$, $Y = \ln[-\ln(1-P_f)]$, and the x-intercept is

$$X_0 = \ln\sigma_0 \tag{A5}$$

Based on the reported value of σ_0, the two possible values of X_0 are 1.178 for common logarithm and 2.534 for natural logarithm. Comparing the values with the test data, one realizes that neither of the two values match with the test data value, which actually is about 1.1 (see Fig. 8). But if we evaluate $\log_{10}\sigma_0 = \log_{10}12.6$, we get the reported x-intercept value of 1.1. Therefore, the necessary conclusion is that the common logarithm must have been used for the horizontal axis ($X = \log_{10}(\sigma-\sigma_0)$), while, for some unknown reason, the correction factor $\log_{10}(\log_{10}e)$ was not considered.

To conclude, though not explicitly stated in the literature after 1939, the Weibull's original test data on concrete were plotted using the natural logarithm for the vertical axis and the common logarithm for the horizontal axis. In addition, the correction constant for the use of common logarithm was not considered.

References

[1] Nordic Committee on Building Regulations, 1978, *Recommendation for Loading and Safety Regulations for Structural Design*, Nordic Committee on Building Regulations, Copenhagen.

[2] Melchers, R. E., and Beck, A. T., 2018, *Structural Reliability Analysis and Prediction*, John Wiley & Sons, New York.

[3] Wang, R. Z., Suo, Z., Evans, A. G., Yao, N., and Aksay, I. A., 2001, "Deformation Mechanisms in Nacre," J. Mater. Res., **16**(9), pp. 2485–2493.

[4] Gao, H., Ji, B., Jäger, I. L., Arzt, E., and Fratzl, P., 2003, "Materials Become Insensitive to Flaws at Nanoscale: Lessons From Nature," Proc. Natl. Acad. Sci. U.S.A., **100**(10), pp. 5597–5600.

[5] Kamat, S., Su, X., Ballarini, R., and Heuer, A. H., 2000, "Structural Basis for the Fracture Toughness of the Shell of the Conch Strombus Gigas," Nature, **405**(6790), p. 1036.

[6] Luo, W., and Bažant, Z. P., 2017, "Fishnet Model for Failure Probability Tail of Nacre-Like Imbricated Lamellar Materials," Proc. Natl. Acad. Sci. U.S.A., **114**(49), pp. 12900–12905.

[7] Luo, W., and Bažant, Z. P., 2017, "Fishnet Statistics for Probabilistic Strength and Scaling of Nacreous Imbricated Lamellar Materials," J. Mech. Phys. Solids, **109**, pp. 264–287.

[8] Luo, W., and Bažant, Z. P., 2018, "Fishnet Model With Order Statistics for Tail Probability of Failure of Nacreous Biomimetic Materials With Softening Interlaminar Links," J. Mech. Phys. Solids, **121**, pp. 281–295.

[9] Luo, W., and Bažant, Z. P., 2019, "Fishnet Statistical Size Effect on Strength of Materials With Nacreous Microstructure," ASME J. Appl. Mech., **86**(8), p. 081006.

[10] Weibull, W., 1939, "A Statistical Theory of the Strength of Materials," Royal Swedish Inst. Eng. Res., **151**(15), pp. 1–45.

[11] Daniels, H. E., 1945, "The Statistical Theory of the Strength of Bundles of Threads. I," Proc. R. Soc. Lond. Ser. A Math. Phys. Sci., **183**(995), pp. 405–435.

[12] Fisher, R. A., and Tippett, L. H. C., 1928, "Limiting Forms of the Frequency Distribution of the Largest or Smallest Member of a Sample," Math. Proc. Cambridge Philos. Soc., **24**(2), pp. 180–190.

[13] Bažant, Z. P., and Pang, S.-D., 2007, "Activation Energy Based Extreme Value Statistics and Size Effect in Brittle and Quasibrittle Fracture," J. Mech. Phys. Solids, **55**(1), pp. 91–131.

[14] Bažant, Z. P., Le, J.-L., and Bazant, M. Z., 2009, "Scaling of Strength and Lifetime Probability Distributions of Quasibrittle Structures Based on Atomistic Fracture Mechanics," Proc. Natl. Acad. Sci. U.S.A., **106**(28), pp. 11484–11489.

[15] Bažant, Z. P., and Le, J.-L., 2017, *Probabilistic Mechanics of Quasibrittle Structures: Strength, Lifetime, and Size Effect*, Cambridge University Press, Cambridge.

[16] Bažant, Z. P., 2005, *Scaling of Structural Strength*, Elsevier, New York.

[17] Bažant, Z. P., 2019, *Fracture and Size Effect in Concrete and Other Quasibrittle Materials*, Routledge, New York.

[18] Le, J.-L., and Bažant, Z. P., 2009, "Strength Distribution of Dental Restorative Ceramics: Finite Weakest Link Model With Zero Threshold," Dent. Mater., **25**(5), pp. 641–648.

[19] Le, J.-L., Bažant, Z. P., and Bazant, M. Z., 2011, "Unified Nano-Mechanics Based Probabilistic Theory of Quasibrittle and Brittle Structures: I. Strength, Static Crack Growth, Lifetime and Scaling," J. Mech. Phys. Solids, **59**(7), pp. 1291–1321.

[20] Xu, Z., Ballarini, R., and Le, J.-L., 2019, "A Renewal Weakest-Link Model of Strength Distribution of Polycrystalline Silicon Mems Structures," ASME J. Appl. Mech., **86**(8), p. 081005.

[21] Salviato, M., and Bažant, Z. P., 2014, "The Asymptotic Stochastic Strength of Bundles of Elements Exhibiting General Stress–Strain Laws," Probab. Eng. Mech., **36**, pp. 1–7.

[22] Marchi, B. C., and Keten, S., 2019, "Microstructure and Size Effects on the Mechanics of Two Dimensional, High Aspect Ratio Nanoparticle Assemblies," Front. Mater., **6**, p. 174.

[23] Fuller, R. B., 1961, "Octet Truss," U.S. Patent Serial No. 2,986,241.

[24] Deshpande, V. S., Fleck, N. A., and Ashby, M. F., 2001, "Effective Properties of the Octet-Truss Lattice Material," J. Mech. Phys. Solids, **49**(8), pp. 1747–1769.

[25] Dong, L., Deshpande, V., and Wadley, H., 2015, "Mechanical Response of Ti–6Al–4V Octet-Truss Lattice Structures," Int. J. Solids Struct., **60**, pp. 107–124.

[26] Zhang, X., Vyatskikh, A., Gao, H., Greer, J. R., and Li, X., 2019, "Lightweight, Flaw-Tolerant, and Ultrastrong Nanoarchitected Carbon," Proc. Natl. Acad. Sci. U.S.A., **116**(14), pp. 6665–6672.

[27] Gu, X. W., and Greer, J. R., 2015, "Ultra-Strong Architected Cu Meso-Lattices," Extreme Mech. Lett., **2**, pp. 7–14.

[28] He, Z., Wang, F., Zhu, Y., Wu, H., and Park, H. S., 2017, "Mechanical Properties of Copper Octet-Truss Nanolattices," J. Mech. Phys. Solids, **101**, pp. 133–149.

[29] Pang, S.-D., Bažant, Z. P., and Le, J.-L., 2008, "Statistics of Strength of Ceramics: Finite Weakest-Link Model and Necessity of Zero Threshold," Int. J. Fract., **154**(1–2), pp. 131–145.

[30] Aeppli, A., 1924, "Zur Theorie verketteter Wahrscheinlichkeiten: Markoffsche Ketten Höherer Ordnung," Ph.D. thesis, ETH Zurich, Zurich.

[31] Guennebaud, G. and Jacob, B., 2010, "Eigen V3," http://eigen.tuxfamily.org.

[32] Ayachit, U., 2015, *The Paraview Guide: A Parallel Visualization Application*, Kitware, Inc.

[33] Nitka, M., and Tejchman, J., 2015, "Modelling of Concrete Behaviour in Uniaxial Compression and Tension With Dem," Granular Matter, **17**(1), pp. 145–164.